



SELECTIVE ELECTROCHEMICAL REDUCTION OF CO₂ TO HIGH VALUE CHEMICALS

Grant agreement no.: 851441

Start date: 01.01.2020 – **Duration:** 36 months

Project Coordinator: Dr. Brian Seger - DTU

DELIVERABLE REPORT

| 2.3 REPORT ON PROMISING M-N-C CATALYST ACTIVITY SHOWING PROGRESS TOWARD WP TARGETS | | |
|---|--|----------|
| Due Date | June. 2021 | |
| Author (s) | Wen Ju, Sven Brückner, Peter Strasser | |
| Workpackage | 2 | |
| Workpackage Leader | Peter Strasser | |
| Lead Beneficiary | TUB | |
| Date released by WP leader | 28-06-2021 | |
| Date released by Coordinator | 28-06-2021 | |
| DISSEMINATION LEVEL | | |
| PU | <i>Public</i> | X |
| PP | <i>Restricted to other programme participants (including the Commission Services)</i> | |
| RE | <i>Restricted to a group specified by the consortium (including the Commission Services)</i> | |
| CO | <i>Confidential, only for members of the consortium (including the Commission Services)</i> | |
| NATURE OF THE DELIVERABLE | | |
| R | <i>Report</i> | X |
| P | <i>Prototype</i> | |
| D | <i>Demonstrator</i> | |
| O | <i>Other</i> | |

| SUMMARY | |
|--|---|
| Keywords | <i>CO₂-to-CO, M-N-C catalysts, 90% FE_{CO} at 400 mA cm⁻²</i> |
| Abstract | This deliverable reports the progress in electrochemical CO ₂ -to-CO conversion in the project-modified MEA cell, using the metal-nitrogen doped carbon (M-N-C) as the catalyst. By adjusting the operation condition, the performance reaches over 90% faradaic CO efficiency at 400 mA cm ⁻² , showing progress to WP target. |
| Public abstract for confidential deliverables | This deliverable describes our recent progress in electrochemical CO ₂ reduction based on the previously reported performance. |

| REVISIONS | | | |
|------------------|-------------|-------------------|-----------------|
| Version | Date | Changed by | Comments |
| 0.1 | 27-06-2021 | Wen Ju | |
| | | | |

REPORT ON PROMISING M-N-C CATALYST ACTIVITY SHOWING PROGRESS TOWARD WP TARGETS

CONTENT

| | | |
|---|---------------------------------|---|
| 1 | Introduction | 4 |
| 2 | Scope | 4 |
| 3 | Results and Discussion..... | 5 |
| 4 | Conclusion and future work..... | 6 |
| 5 | References | 7 |
| 6 | Appendix..... | 8 |

1 INTRODUCTION

The metal-nitrogen doped carbon (M-N-C) is a promising candidate for electrochemical CO₂ reduction (ECO2R). Among those M-N-C catalysts, the nickel-based one (Ni-N-C) shows high selectivity for CO formation,¹⁻⁵ hence, attracted significant attention. However, deploying the Ni-N-C candidates in large-scale GDL still faces technical challenges due to their structural complexities. For instance, we reached over 85% FE_{CO} at 250 mA cm⁻²; however, the CO selectivity can hardly be maintained when approaching higher current densities (≥ 300 mA cm⁻², MS2). The flooding and salt issues arise at high current densities, lowering the CO₂ accessibility (to in-pores active sites) and switching the selectivity towards the hydrogen evolution reaction (HER). In our recent study, by tuning the reaction condition, we can maintain over 90% FE_{CO} at 400 mA cm⁻² current densities, showing progress toward the WP target.

2 SCOPE

As reported in MS2, we reached over 85% FE_{CO} at 250 mA cm⁻², and the required cell potential was about 3.4 V. In this approach, we modified several parameters in our measurement protocol to improve the ECO2R performance. We tuned the CO₂ inlet flow rate (to fulfill high currents CO₂ consumption)⁶, used S-ionomer as the catalyst binder (for a better catalyst - membrane contact), and changed the cell temperature. Other parameters were kept identical to our earlier reports. In this context, we stress the impact of the reaction temperature.

Our testing platform configuration is illustrated in Figure 1. We control and sense the temperature of the anolyte, and the anolyte flow serves as the heating source of the MEA cell. The ECO2R performance at T1, T2, T3, and T4 has been tested.

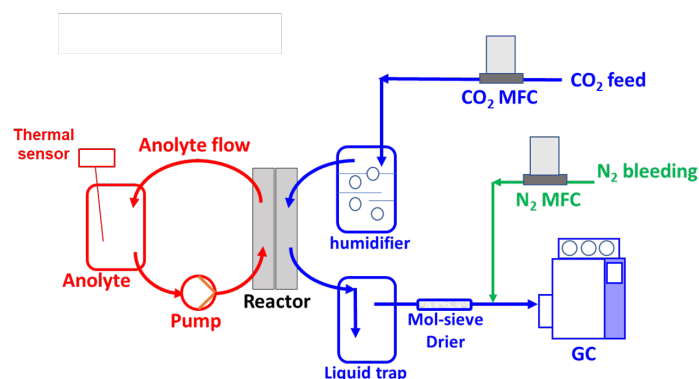


Figure 1: Illustration of our MEA testing platform for temperature effect. A heating mantle and a thermal sensor are deployed to control the anolyte temperature. Here, the anolyte (A M KCHO₃) is pumped into the cell (with a B mL min⁻¹ flow rate) as the heating source for the MEA cell. IrO₂ GDE (Dioxide Materials) is used as the anode material, whereas the Sustainion membrane is used. Next, L mg cm⁻² loading NiNC-MOF catalyst with X wt% S-ionomer is sprayed on DeNora DN908 GDL. In the cathode chamber, no catholyte is applied. Instead, humidified CO₂ flow is driven by a mass flow controller (MFC, Bronkhorst) with a C mL min⁻¹ flow rate. The product stream out from the cell is purged through the condenser (25 °C) and a mole-sieve drier; then mixed with a N₂ bleeding (D mL min⁻¹) line for GC analysis. Production quantitative analysis is listed in Appendix.

3 RESULTS AND DISCUSSION

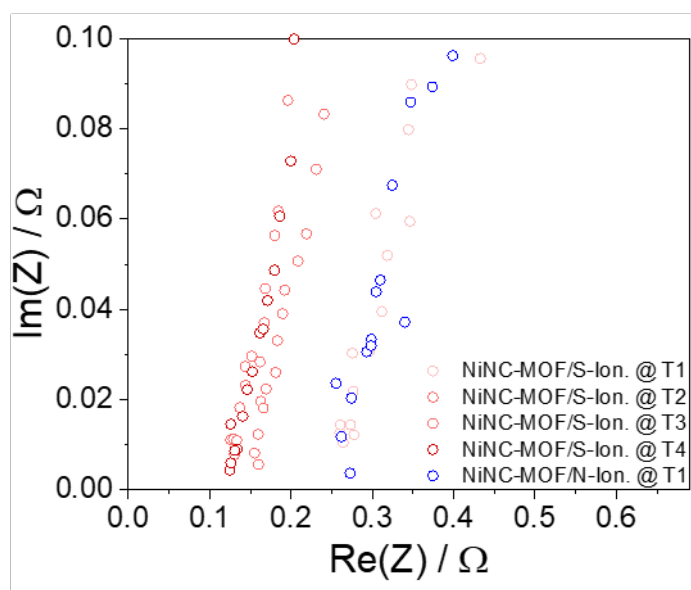


Figure 2: Nyquist plots of our studied GDLs (0 A current) at different temperatures. Catalyst loading: $L \text{ mg cm}^{-2}$ NiNC-MOF catalyst on DN908 GDL. The blue point is an identical GDL but using N-ionomer.

We measure the cell resistance using the GEIS module at 0 A current before the catalytic performance screening. The frequency is set from 500,000 to 0.1 Hz. The Nyquist impedance (at 0 A) of 4 different operation temperatures (T1, T2, T3, and T4) is presented in Figure 2. Herein, we cite the GDL ($L \text{ mg cm}^{-2}$ catalyst loading with N-ionomer) reported in MS2 as the reference. At T1, the S-ionomer shows no apparent difference from the N-ionomer binder in charge conductivity. Notably, the rising cell temperature (by heating the anolyte flow to T2 or higher) could largely lower the cell charge resistance.

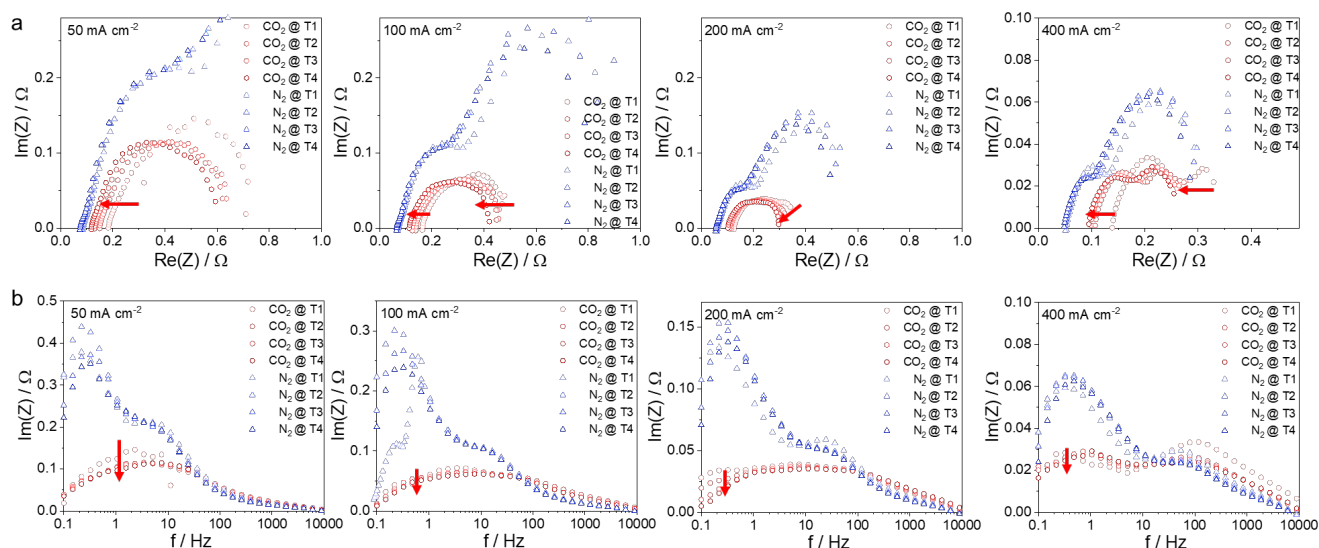


Figure 3: a. Nyquist plots, and b. impedance as a function of the frequency of our MEA cell at various temperatures and current densities.

To further determine the cell ionic resistance under operation conditions, we carried out the GEIS protocol at various temperatures while keeping a constant current density. Figure 3 row-a displays the Nyquist plot under those conditions. Here, the blue profiles are the Nyquist plots with pure N₂ feeding (to force the H₂O/OH⁻ in-membrane transfer) as control measurements. At all given current densities, both cell charge and ion resistance decrease at *SELECTCO2 Deliverable Report D.2.3. – Report on promising M-N-C catalyst activity showing progress toward WP targets - 5* 28/06/2021 – Version 1

increased temperatures. It is noteworthy that the cell suffers higher ion resistance without CO₂ feeding. This implies that the CO₂-related species (CO₂/HCO₃⁻/CO₃²⁻) are favored in the cathodic chamber, presumably in the Sustainion anion exchange membrane as well.

Figure 3 row-b plots the cell impedance (GEIS) as a function of frequency. Herein, compared to the profiles of N₂ feeding, the low-frequency region seems to correspond to the movement of CO₂-based active species inside the MEA.⁷ Obviously, those mass transfers could be accelerated at raising the temperature, which could be beneficial for the CO₂ electrolysis performance.

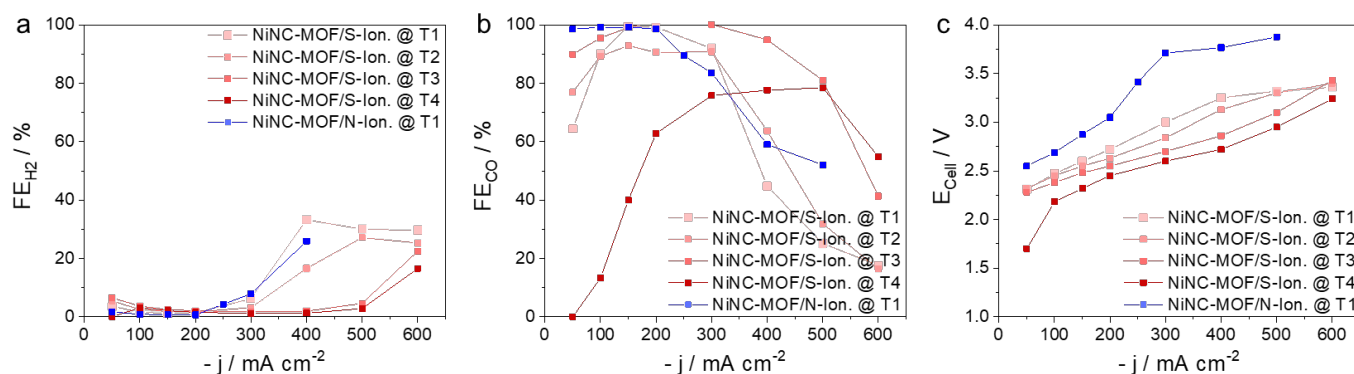


Figure 4: ECO2R performance of all NiNC-MOF-GDLs tested in MEA cell at different temperatures. **a.** Faradaic efficiency of H₂, **b.** faradaic efficiency of CO, and **c.** cell potential without IR-correction at various current densities. Catalyst loading: L mg cm⁻² on DN908 GDL.

The ECO2R performance screening is performed from 50 mA cm⁻² to 600 mA cm⁻² current densities, with an increment of 50 or 100 mA cm⁻². The current density was kept stationary for 15 min for each step, while the GC analysis was taken at minute 14 in the step. In Figure 4a and b, we compare the faradaic efficiency of H₂ and CO at various reaction temperatures. At T1, the GDL using S-ionomer binder (MS2 reference) displays a similar performance as the N-ionomer doped one (reference from MS2). The FE_{H₂} raises to 40% at 400 mA cm⁻², simultaneously draws the FE_{CO} below 60%. Remarkably, the FE_{CO} could be maintained at elevated temperatures. Approximately 95% FE_{CO} (FE_{H₂} < 5%) could be achieved at 400 mA cm⁻² when the anolyte is heated to T3. However, up to T4, the total faradaic efficiency counts below 80%, indicating the product crossover through the membrane. Next, we turn to Figure 4c, the cell voltage (without IR-correction) to drive each current density. The rising (anolyte) temperature could gradually decrease the potential demand. Compared to T1, electrolysis at T3 could reduce 500 mV cell voltage (1000 mV less than MS2). According to our experimental observation, we speculate that the temperature could boost CO₂ transfer into the catalyst layer and the HCO₃⁻/CO₃²⁻ removal through the membrane, further benefitting CO₂-to-CO conversion. **All those verify the performance progress toward WP targets.**

4 CONCLUSION AND FUTURE WORK

In this framework, we performed the ECO2R in the MEA-cell by tuning the reaction temperature. Improved CO activity could be achieved at elevated temperatures, and in our context, an optimal performance (> 90% FE_{CO} at 400 mA cm⁻², E_{Cell} < 2.8 V) occurs at T3. Based on, but limited in, our experimental protocol and observation, we can only attribute this to the temperature-boosted transfer of CO₂-related species. Aside from the mass transfer, other factors such as the temperature-affected GDL humidity, temperature-lowered activation energy, and temperate boosted CO desorption deserve systematic investigation (in collaboration with DTU and EPFL). Moreover, beyond the progress we achieved in CO activity, TUB will collaborate with DTU, TUD, US, and DENO to improve the performance stability.

5 REFERENCES

- 1 Varela, A. S., Ju, W. & Strasser, P. Molecular Nitrogen–Carbon Catalysts, Solid Metal Organic Framework Catalysts, and Solid Metal/Nitrogen-Doped Carbon (MNC) Catalysts for the Electrochemical CO₂ Reduction. *Advanced Energy Materials* **8**, 1703614, doi:10.1002/aenm.201703614 (2018).
- 2 Varela, A. S. *et al.* Electrochemical Reduction of CO₂ on Metal-Nitrogen-Doped Carbon Catalysts. *ACS Catalysis* **9**, 7270-7284, doi:10.1021/acscatal.9b01405 (2019).
- 3 Möller, T. *et al.* Efficient CO₂ to CO electrolysis on solid Ni–N–C catalysts at industrial current densities. *Energy & Environmental Science*, doi:10.1039/C8EE02662A (2019).
- 4 Ju, W. *et al.* Understanding activity and selectivity of metal-nitrogen-doped carbon catalysts for electrochemical reduction of CO₂. *Nature Communications* **8**, 944, doi:10.1038/s41467-017-01035-z (2017).
- 5 Jiang, K. *et al.* Isolated Ni single atoms in graphene nanosheets for high-performance CO₂ reduction. *Energy & Environmental Science* **11**, 893-903, doi:10.1039/C7EE03245E (2018).
- 6 Ma, M. *et al.* Insights into the carbon balance for CO₂ electroreduction on Cu using gas diffusion electrode reactor designs. *Energy & Environmental Science* **13**, 977-985, doi:10.1039/D0EE00047G (2020).
- 7 Bienen, F. *et al.* Revealing Mechanistic Processes in Gas-Diffusion Electrodes During CO₂ Reduction via Impedance Spectroscopy. *ACS Sustainable Chemistry & Engineering* **8**, 13759-13768, doi:10.1021/acssuschemeng.0c04451 (2020).

6 APPENDIX

Set up and experimental details

A Shimadzu 2014 on-line GC is utilized for product quantification. The gas stream is separated by the Hayesep Q column and then analyzed by the TCD (Thermo Conductivity Detector) and FID (Flame Ionization Detector). The TCD detects the volume percentage (%vol) of the H₂ product and the N₂ bleeding, whereas the FID measures the CO after methanization. On the M-N-C type catalyst, no liquid product is expected during the electrolysis.^{3,4}

Products distribution analysis

The actual total gas flow rate into the GC sample loop could be calculated as Eq. 1.

$$\dot{V}_{Total} = \dot{V}_{N_2} + \dot{V}_{Reaction} = \frac{\dot{V}_{N_2}}{C_{N_2}} \quad \text{Eq. 1}$$

| | | |
|------------------------|---|-------------------------|
| \dot{V}_{Total} : | actual total stream flow rate | (mL min ⁻¹) |
| \dot{V}_{N_2} : | defined N ₂ bleeding flow rate | (mL min ⁻¹) |
| $\dot{V}_{Reaction}$: | actual product stream flow rate | (mL min ⁻¹) |
| C_{N_2} : | N ₂ concentration detected by GC | (%vol) |

Calculations of the production rate (Eq. 2), partial current density (Eq. 3), and faradaic efficiency (Eq. 4) are given below.

$$\dot{n}_{Product} = \frac{\dot{V}_{Total} \times C_{Product}}{A \times V_{MOL}} \quad \text{Eq. 2}$$

| | | |
|-----------------------|--|---|
| $\dot{n}_{Product}$: | geometric reaction rate of each product | (mol s ⁻¹ cm ⁻²) |
| $C_{Product}$: | concentration of each product detected by GC | (%vol) |
| A : | geometric area of the electrode | (cm ²) |
| V_{MOL} : | volume of gas per molar at ATM | (mL mol ⁻¹) |

$$j_{Product} = \dot{n}_{Product} \times F \times z \quad \text{Eq. 3}$$

| | | |
|-----------------|---|------------------------|
| $j_{Product}$: | partial current density of each product | (mA cm ⁻²) |
| F : | faradaic constant | (C mol ⁻¹) |
| z : | charge transfer of each product | |

$$FE_{Product} = \frac{j_{Product}}{j_{Total}} \times 100\% \quad \text{Eq. 4}$$

| | | |
|------------------|-------------------------------------|------------------------|
| $FE_{Product}$: | faradaic efficiency of each product | (%) |
| j_{Total} : | total current density | (mA cm ⁻²) |